Journal of Directed Energy, 1, Winter 2006, 275–281

Eight-Watt Coherently Phased Four-Element Fiber Array

Jesse Anderegg, Stephen Brosnan, Dennis Hammons, Hiroshi Komine, Mark Weber, and Michael Wickham*
Northrop Grumman Space and Technology, Redondo Beach, California 90278

A four-element fiber array has been constructed to yield 8 W of coherently phased, linearly polarized light energy in a single far-field spot. Each element consists of a 2-W, single-mode fiber-amplifier chain. Phase control of each element is achieved with a lithium–niobate phase modulator. A master laser provides a linearly polarized, narrow-linewidth signal that is split into five channels. Four channels are individually amplified by using polarization maintaining fiber power amplifiers. Frequency broadening of the signal is necessary to avoid stimulated Brillouin scattering. The fifth channel is used as a reference arm. It is frequency shifted and then combined interferometrically with a portion of each channel's signal. Detectors sense the heterodyne modulation signal, and an electronics circuit measures the relative phase for each channel. Compensating adjustments are then made to each channel's phase modulator. The stability of the optical train is an essential contributor to its success. A state-of-the-art interferometer was built with mountless optics. A lens array was constructed by using nanopositioning tolerances, where each lens was individually aligned to its respective fiber to collimate its output and point it at a common far-field spot. This system proved to be highly robust and handled any acoustic perturbations.

KEYWORDS: Fiber amplifier, Phase control, Phased array

1. Introduction

Northrop Grumman Corporation has been engaged in fiber-amplifier research for the past four years and has been pursuing the goal of a high-power, fiber-amplifier phased array. We report in this paper on the successful demonstration of a robust phased array of four 2-W ytterbium fiber amplifiers.

2. Experiment

The basic experiment design is shown in Fig. 1. The master laser is an external-cavity semiconductor laser whose drive current is modulated so as to produce a spectrally broadened output, which is needed to suppress stimulated Brillouin scattering (SBS) in the amplifier. Power from the master laser is isolated and then divided among five paths, one reference arm and four amplified signal arms. Light in the reference arm is frequency shifted in an

---

Received February 3, 2003; revision received March 25, 2004.

*Corresponding author; e-mail: michael.wickham@ngc.com.

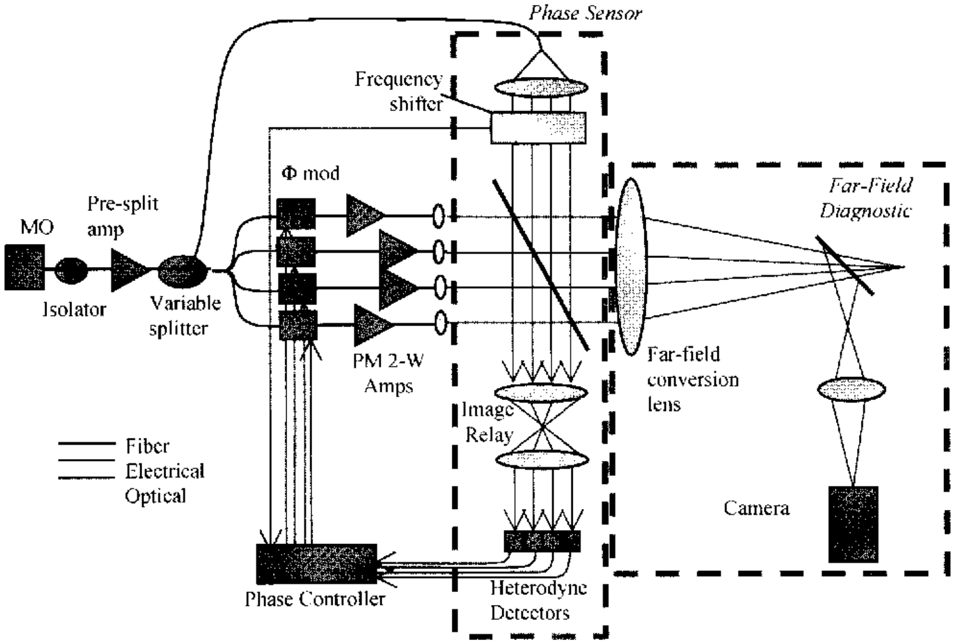

Fig. 1. Phase-locked fiber array experiment schematic.

acousto-optic Bragg cell. A sample of each signal beam is interfered with the reference beam to generate a heterodyne beat waveform that is used to measure the phase of that arm relative to that of the reference arm. The phase controller performs the phase measurement in fully parallel electronics and adjusts the phase of each arm with a control voltage to individual lithium–niobate waveguide phase modulators. The far-field diagnostic consists of a far-field conversion lens, a beamsplitter, and a digital video camera outfitted with a zoom microscopic lens system.

The interferometer plate was the heart of the experiment. A photograph of the finished plate is shown in Fig. 2. The incoming reference light was collimated and then frequency shifted in the Bragg cell. The beam was then shaped to match the size and aspect ratio of the linear four-element array by expanding first with a telescope and then with a prism beam expander. The signal input and phase-sensor output beams were handled by fibers contained in silicon v-groove arrays, as described below. Collimation and focusing lenses for these arrays were positioned with precise tolerances by using visual feedback from the far-field diagnostic camera system. The critical optical alignment of the interferometer components was achieved with an align-and-lock technique. Once aligned, no adjustments were required and the system alignment remained stable.

The assembly of the four-element lens array was the most challenging task due to precise positioning requirements. Two views of the v-groove array are shown in Fig. 3. The 48-v-groove assembly had a pitch of 250 μm and centration errors <0.5 μm. Polarization-maintaining fibers with parallel alignment populated every 12th groove to provide a 3-mm fiber-to-fiber spacing. The fiber ends were polished as a group at 8 deg to minimize feedback. No antireflection coatings were applied. The v-groove was attached to a 3.7-deg ramp so that the output of the array would be parallel to the table. The focal length of the lenses was 6.7 mm and their diameter was 2.5 mm.

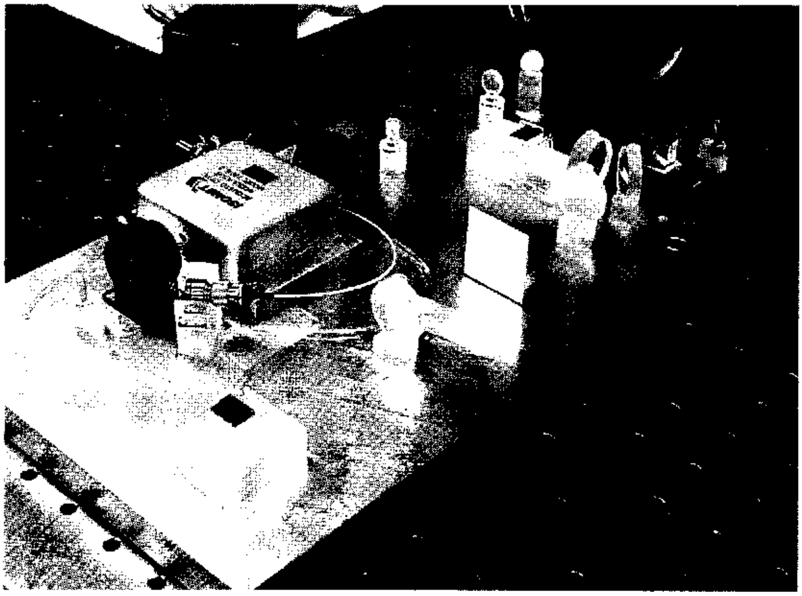

Fig. 2. Interferometer plate photograph.

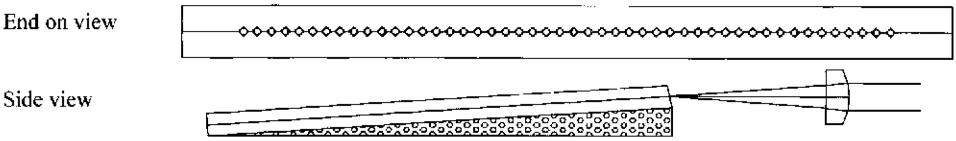

Fig. 3. Views of silicon v-groove array and support ramp.

The collimating lenses were aligned so that all four beams coincided in the far field within 10% of the far-field spot size, as shown in Fig. 4. This required positioning of the lenses to submicron accuracy while observing the far-field video diagnostic. The lens and its support structure were positioned with a hybrid mechanical/electrostrictive XYZ positioner. The lens alignment resulted in excellent overlap of the far-field centroids of the four beams, as shown.

Once the interferometer plate was assembled and aligned, it was integrated with the rest of the optical and electrical components of the experiment. Other components included the master laser with isolator, optical amplifiers, phase adjusters, and phase control electronics. The master laser was an external-cavity semiconductor laser, made by Sacher Laser, had an output of 30 mW, and was operated at 1,080 nm. All of the fiber amplifiers were purchased from IPG Photonics. A variable power splitter is shown after the 1-W preamplifier, which allowed the reference and test legs to be power balanced.

Path length matching was required to ensure that the length mismatch between reference and test legs' optical paths were within the coherence length of the master laser. The required spectral width to suppress SBS was 1 GHz, which required the path length to be matched within 3 cm. This was achieved by using mode-locked laser pulses at 1,064 nm to probe the reference and signal arms. The amplifiers were operated at a low level to allow probe laser transmission. The path length differences were determined by measuring the relative time of arrival of pulses at the detector plane.

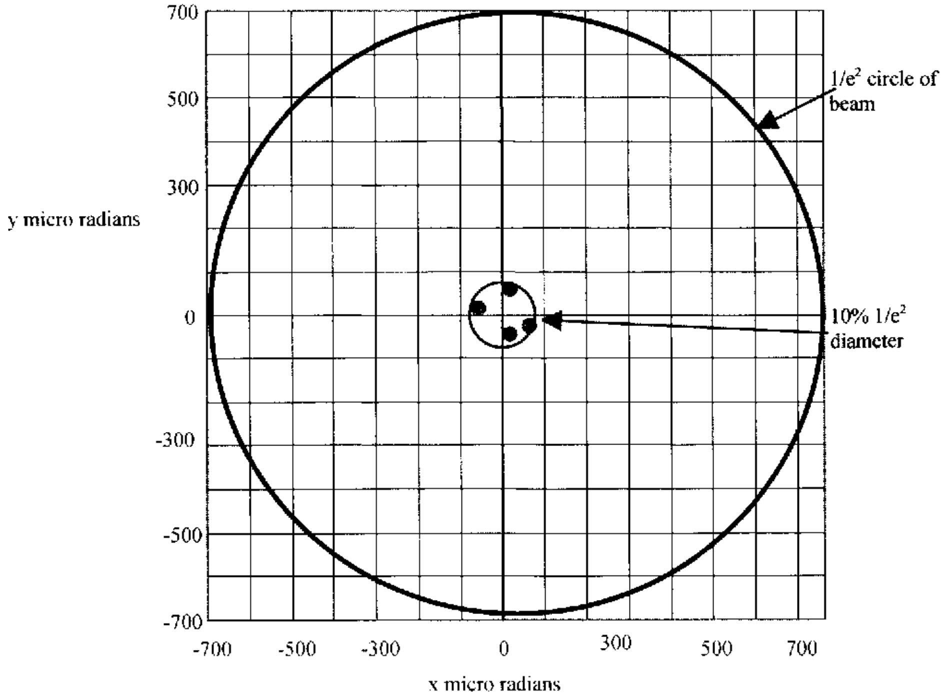

Fig. 4. Far-field centroids for the four-array elements, as compared to diameter of an element's beam.

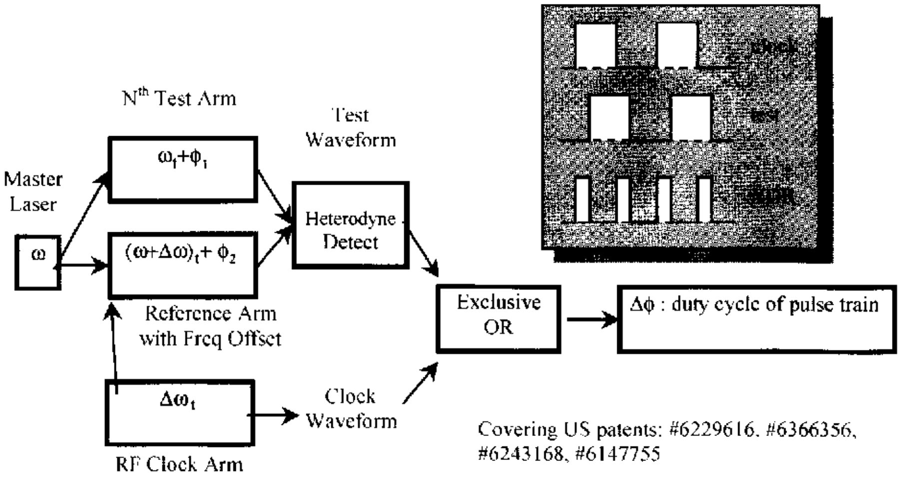

Covering US patents: #6229616, #6366356, #6243168, #6147755

Fig. 5. Phase-sensing electronics concept.

The phase control electronics is another important contributor to the success of this work. The concept of the heterodyne phase-sensor measurement is shown in Fig. 5. A heterodyne beat signal results from the interference of the reference with each signal. This sinusoid waveform is squared up by passing it through a saturating amplifier and results in the "test" waveform shown in the inset of Fig. 5. A similar square waveform is created from a sample of the radio frequency (RF) drive to the frequency shifter, shown as the "clock." The phase difference between these waveforms is identical to the optical phase difference between the test and reference arms. An exclusive-OR function is performed between the clock and each test leg signal. The measured phase difference is linearly proportional to the area of this

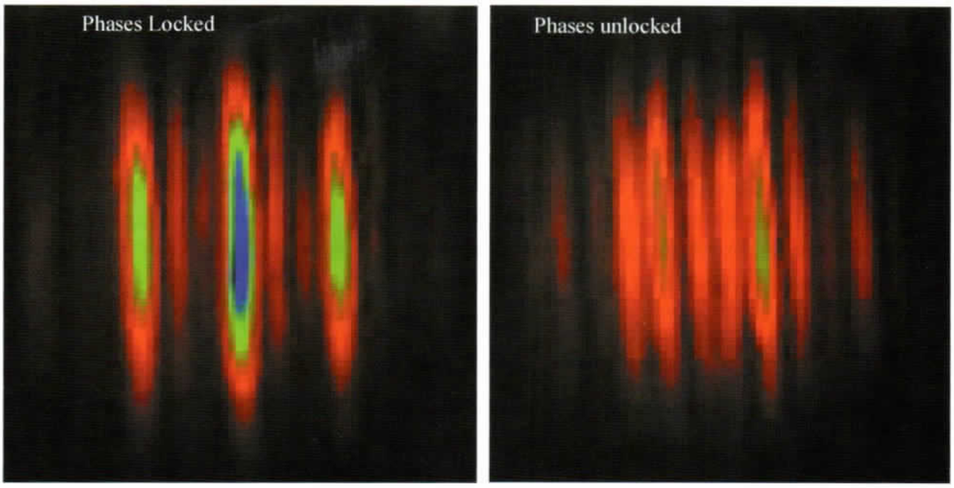

Fig. 6. Images showing far-field pattern from four fiber amplifiers, both locked and unlocked.

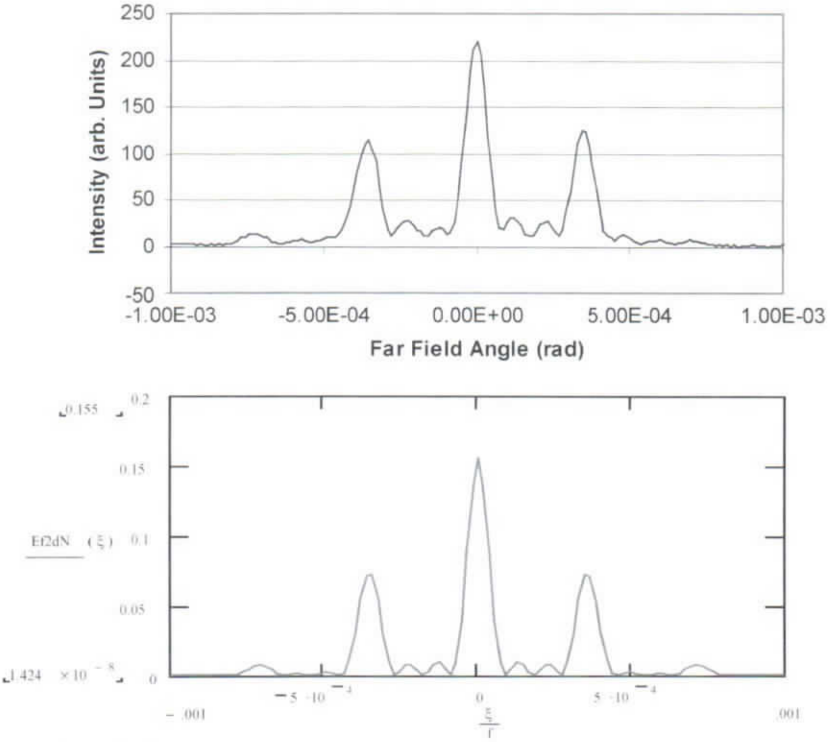

Fig. 7. Measured and predicted far-field horizontal fringe profiles.

XOR function result. A voltage proportional to this value is sent to the phase adjuster for each test leg to correct the phase of that leg. In this way, all of the output phases are exactly aligned. When the locking loop is closed, we observe less than 7 mrad of rms phase noise.

The four coherently combined beams were displayed by the far-field diagnostic camera, and the fringe pattern was recorded. Figure 6 shows the fringe pattern with and without the phase control electronics engaged. When the loop is closed, the fringes are stable and the peak intensity is maximized. In fact, the fringes remain stable even when the fiber is actively manipulated by hand, thereby demonstrating the robust phase locking that we have achieved. With the locking loop open, the fringes are unstable and the peak intensity is low. Hand manipulation of the fiber makes the fringes highly unstable.

The side lobes are the result of the interlens separation and the fact that the lens areas are not uniformly illuminated. The profile of the fringes has been taken by capturing a horizontal slice through a digitized image and is shown by the top curve of Fig. 7. The bottom curve shows a theoretical prediction of the profile. Clearly, the agreement is quite good.

3. Conclusion

We have successfully demonstrated a phased array of fiber amplifiers, yielding 8 W from an array of four elements. Our phase-sensing and control electronics provided robust locking against acoustic noise and active manipulation of the fibers. The electronics is fully parallel and shows no scaling bottlenecks. We feel that this demonstration shows that large, high-power fiber arrays are feasible.

4. Acknowledgments

This work was sponsored by the Air Force under the Laser Engineering and Technology Support (LETS) program, Contract F29601-98-D-0033.

The Authors

Mr. Jesse Anderegg is a Senior Member of the Technical Staff at Northrop Grumman Space Technology. Since 1999, he has worked to develop high-power fiberoptic amplifiers, including advanced side-pumping and end-pumping techniques of dual-clad rare-earth-doped fibers and coherent combination of multiple-fiber lasers. Mr. Anderegg received his Master's degree in Physics Instrumentation from the University of Utah.

Dr. Stephen J. Brosnan is a Senior Scientist at Northrop Grumman and since 1997 has worked to develop high-power fiberoptic amplifiers, including a comprehensive fiber amplifier numerical model. His research interests over 25 years have included frequency conversion techniques and 3-dimensional Doppler velocimetry. His doctoral work at Stanford University was in the field of nonlinear optics, emphasizing parametric and Raman frequency conversion. His paper on optical parametric oscillator threshold and linewidth studies has been widely referenced.

Dr. Dennis Hammons is a Senior Member of the Technical Staff at Northrop Grumman Space Technology. His areas of research include the development of high-power fiber amplifiers and solid-state laser for directed energy and LADAR applications.

Dr. Hiroshi Komine is a Senior Staff Engineer at Northrop Grumman Corporation. Since obtaining a doctorate from Stanford University in the field of lasers and nonlinear optics, he has carried out more than 28 years of research and development in high-power solid-state lasers and phased-array fiber laser systems, linear/nonlinear optical devices for wavelength conversion, beam combining and clean-up, coherent/incoherent lidars for obstacle avoidance, laser flowfield velocimetry, and active tracking. Since 1997, he has been a technical lead on high-power laser system concepts and architectures.

Mr. Mark Weber is a Member of the Technical Staff at Northrop Grumman Space Technology. Since 1986, he has worked to develop specialized power and control electronics for solid-state lasers. This has ranged from advanced high-power laser diode power supplies to the RF and digital control electronics used in coherent combination of multiple-fiber lasers. Mr. Weber received his B.S.E.E. from California State, Long Beach.

Dr. Michael Wickham is a Senior Scientist at Northrop Grumman and is the High Power Fiber Technical Lead at Northrop Grumman. He specializes in laser physics, photonics, optical diagnostics, and experimental plasma physics. He has published more than two dozen papers in related areas and has 17 patents. His doctoral work at the University of California at Irvine was in the field of controlled thermonuclear plasma physics.